The BRDFs of Land Surfaces Estimated from the Airborne POLDER Data

Y. Kawata
(*Environmental Information Research Laboratory Kanazawa Institute of Technology, Ogigaoka 7—1, Nonoichi, Ishikawa 921, Japan*)

K. Takemata
(*Department of Electrical Engineering Kanazawa Technical College, Hisayasu 2—270, Kanazawa, Ishikawa 921, Japan*)

T. Yonekura
(*Environmental Information Research Laboratory Kanazawa Institute of Technology, Ogigaoka 7—1, Nonoichi, Ishikawa 921, Japan*)

Abstract In this study, the estimation of the Bidirectional Reflectance Distribution Functions (BRDFs) for selected land cover types was made by using the airborne POLDER image data. The main results in this study can be summarized as follows:

(1) We presented an specially improved atmospheric correction algorithm, applicable to a framed image data by the POLDER sensor. The terrestrial images measured successively by the airborne POLDER with a different viewing angle were converted to a series of surface albedo images by our atmospheric correction method, in which the multiple scattering were taken into account for.

(2) Then, the spectral BRDFs for selected 21 target areas, including the cover types of River, Pond, City, Road, Forest were estimated from using successive albedo images. It was found that the BRDF for water surfaces follow a Lambertian law at both 550nm, 650nm and at 850nm. It was also found that the BRDFs for vegetated surfaces are more or less isotropic at 550nm and 650nm, but they are anisotropic at 850nm. The fitting parameters of the empirical BRDF law for all of target surfaces were presented.

Key words POLDER, BRDF, Atmospheric correction, Multiple scattering

1 INTRODUCTION

The POLDER (POLarization and Directionality of the Earth Reflectance) instrument is scheduled for launch in August, 1996 on the Japanese ADEOS (ADvanced Earth Observing System) platform by the National Space Development Agency (NASDA). The POLDER is designed to measure both the polarized and directional solar radiation in the visible and near—infrared spectral bands reflected by the earth—atmosphere system[1]. To prepare for the spaceborne experiment, the airborne version of POLDER has already made measurements over lands and seas[2,3]. The "La Crau campaign" was conducted in the southeast of France on June 17, 1990. In this study, we consider only a subset of a large La Crau data set to estimate the Bidirectional Reflectance Distribution Functions (BRDFs) for selected surface targets.

2 LA CRAU DATA

The airborne POLDER data over "La Crau" used in this analysis consists of over 55 frame images, and the flight altitude was 5900 m. The airplane pass was along near the east—west line and the moving direction of airplane was roughly toward the sun's direction. The airborne POLDER's image consists of 384 × 288 pixels, corresponding to an actual ground area of 15km × 11km. The footprint of a pixel is approximately an area of 37m × 37m. The ranges of the viewing zenith angles are up to ±52° in the crosstrack direction and up to ±44° in the alongtrack direction. The solar zenith and the azimuthal angles

at the time of the observation were $\theta_0 = 43^\circ$ and $\phi_0 = 104^\circ$, respectively. Only the reflectance data at the wavelengths of 550nm, 650nm and 850nm were analized in this study.

3 ATMOSPHERIC CORRECTION

Because the atmospheric correction algorithm used in this study was described in our previous paper[4,5], we repeat it here only briefly. For the airborne frame image data, we need to evaluate the internal radiation field. Let us assume an incident solar flux πF illuminates a plane parallel atmosphere from the direction of (μ_0, ϕ_0), where μ_0 and ϕ_0 are the cosine of the solar zenith angle θ_0 and the solar azimuth angle, respectively. In order to deal with the internal radiation field, we divide such the atmosphere into two layers at the aircraft altitude, namely, the atmosphere above the aircraft (Layer a) and the atmosphere below the aircraft (Layer b). Each layer is assumed to be horizontally homogeneous atmosphere. In this study land surfaces are assumed to be characterized by a target albedo A_t, and a mean background albedo $\bar{A}$. Let the atmospheric optical thickness, reflection and transmission functions of Layer a be τ_a, R_a and T_a, respectively. Similarly, let those of Layer b be τ_b, R_b and T_b, respectively. The internal radiance I_u at POLDER aircraft level in the direction of (μ, ϕ) can be expressed by Eq. (1), in terms of the upwelling diffuse radiation U at the aircraft altitude.

$$I_u(\mu, \mu_0, \phi - \phi_0) = \mu_0 U(\mu, \mu_0, \phi - \phi_0) F \quad (1)$$

For given atmospheric parameters, such as the optical thickness, single scattering albedo and the turbidity factor of the atmospheric layers, we can compute U by using the doubling and adding method[6]. The explicit formulations for computing U in terms of R_a, T_a, R_b and T_b and A_t, $\bar{A}$ were given by kawata *et al.*[4].

Considering a single reflection by a target with an albedo of A_t and up to double reflections by the background with a mean albedo of $\bar{A}$, the internal radiance I_u can be expressed approximately in terms of A_t and $\bar{A}$ by Eq. (2),

$$I_u = (s \cdot \bar{A} + t) A_t + (p - s) \bar{A}^2 + (q - t) \bar{A} + r \quad (2)$$

where p, q, r, s and t are radiance coefficients. Then, the mean internal radiance $\bar{I}_u$ can be given by assuming $A_t = \bar{A}$ in Eq. (2) as follows,

$$\bar{I}_u = p \cdot \bar{A}^2 + q \cdot \bar{A} + r \quad (3)$$

These radiance coefficients p, q, r, s and t can be computed without difficulty by applying a least square method in Eq. (2)—(3), using pre-computed values of I_u and $\bar{I}_u$ for various values of $\bar{A}$ and A_t from Eq. (1)[4]. The atmospheric correction algorithm is given as follows: 1) We first make radiance coefficients p, q, r, s and t for different viewing directions, based on multiple scattering calculations in the earth's atmosphere/ground system. These values are stored in the files as radiance coefficient tables. 2) Then we compute the mean background albedo around the target by Eq. (3) from the observed mean radiance value averaged over a certain background area of the target pixel within the frame image. 3) The radiance coefficients for the corresponding viewing direction of the target pixel are interpolated from the radiance coefficient table files in step 1). 4) The target albedo computation is performed by Eq. (2) from the observed target radiance value, together with the mean background albedo value $\bar{A}$ estimated in step 2). 5) Repeat from steps (2) to (4) for all target pixels.

4 ATMOSPHERIC MODEL

The estimation of the surface albedos requires information on atmospheric parameters at the time of the observation. Ground-based measurements of the atmosphere before and during the airborne flight over La Crau area were given and they can be summarized as follows[2]: 1) Aerosol optical thicknesses were $\tau = 0.400$ at 550nm and $\tau = 0.201$ at 870nm, respectively, from sun photometer measurements. 2) The refractive index of aerosols was estimated to be $m = 1.50 - 0.005i$ at 550nm and 850nm from the sky radiance measurements. 3) The aerosol size distribution was derived from aureole measurements.

We adopted above atmospheric optical parameters in our atmospheric correction. Since we found the slope of the observed size distribution is very similar to that of Junge type aerosol model with $v = 3$, we adopted Junge type aerosols with $v = 3$ as an appropriate aerosol model and its explicit form is given by Eq. (4)

$$\begin{aligned} n(r) &= C \cdot 10^{v+1} \quad \text{for } 0.02\mu m \leq r \leq 0.1\mu m \\ n(r) &= C \cdot r^{-(v+1)} \quad \text{for } 0.1\mu m \leq r \leq 10\mu m \\ n(r) &= 0 \quad \text{for } r < 0.02\mu m \text{ and } r > 10\mu m \end{aligned} \tag{4}$$

where $n(r)$ is the number of particles of radius r per unit increment in radius r. Because values of the molecular optical thickness at 550, 650nm and 850nm were not given in[2], we adopted the molecular optical thickness values based on the standard model atmosphere of Lowtran 6 (Midlatitude, Spring—Summer model)[7]. Lambert's law was assumed for a surface reflection. Using above mentioned atmospheric and surface parameters, we have computed radiance coefficients tables which are needed in the atmospheric correction. Then, we applied our atmospheric correction algorithm to 55 POLDER scenes and we obtained three spectal albedo images for each of 55 scenes.

5 ESTIMATION OF BRDFS

In our previous paper we selected three target areas (River Water, Rice Field, and Forest) whose locations lie along near the flight pass and the estimation of the BRDFs for them was made[4]. In this paper, we extend the previous analysis by incresing the number of target areas from 3 to 21 (including 8 land cover categories: River, Pond, City, Road, Rice Field, Forest, Orchard, Vine Yard, and Warsh). In the analysis, we shall use Deuzé's BRDF model[2] for the target areas. His simple empirical reflectance model is expressed by the sum of an isotropic contribution, a function accounting for the brightening to the limb viewing (c_1), and a function accounting for the maximum in the sun's direction (c_2).

$$A_t' = k_0 + c_1 \cdot k_1 + c_2 \cdot k_2 \tag{5}$$

where,

$$c_1 = 1 - \mu\mu_0 \tag{6}$$

$$c_2 = [\min(0, \cos\Theta)]^2 - 1 \tag{7}$$

and A_t' is the target albedo, Θ is a scattering angle. The three coefficients k_0, k_1 and k_2 are obtained with a least square fit on estimated target albedo values for different viewing angles.

Table 1 shows the values of these three coefficients, the root mean square of difference between A_t and A_t' and the coefficient of determination for each of 21 target surface covers. We can judge that the degree of model fitting is generally good for non—water surface covers, because of their high coefficients of determination $R^2 > 0.7$. On the other hand, Deuzé's BRDF model is not good for water surface covers, i.e., River and Pond, which have low values of R^2.

Table 1 Values of fitting parameters of an empilical BRDF law

Surface	Band[nm]	N_{obs}	K_0	K_1	K_2	σ_{obs}	RMS_{dif}	R^2
River 01	850	13	0.17933	−0.07022	0.00209	0.00032	0.01454	0.03831
	650		0.07870	0.06993	−0.01399	0.00005	0.00504	0.40659
	550		0.12493	0.01301	0.02905	0.00023	0.01679	0.11170
River 02	850	13	0.19131	−0.11395	−0.00951	0.00058	0.01949	0.15753
	650		0.08972	0.00706	−0.03984	0.00033	0.01005	0.54374
	550		0.10727	0.02452	−0.01034	0.00021	0.00918	0.13396
Pond 01	850	16	0.18788	−0.12638	−0.01007	0.00067	0.01892	0.22687
	650		0.07059	0.00942	−0.02470	0.00014	0.00712	0.45666
	550		0.09030	0.04034	−0.02723	0.00014	0.00485	0.75046
Pond 02	850	12	0.22912	−0.20436	0.00374	0.00126	0.02985	0.09405
	650		0.05458	0.02798	−0.02908	0.00011	0.00502	0.73195
	550		0.05349	0.10158	−0.02258	0.00013	0.00577	0.67011

to be continue

Surface	Band[nm]	N_{obs}	K_0	K_1	K_2	σ_{obs}	RMS_{diff}	R^2
City 01	850	15	0.29420	0.45435	0.19689	0.00309	0.00960	0.95766
	650		0.21892	0.19710	0.13655	0.00152	0.00930	0.88031
	550		0.19607	0.02512	0.04347	0.00031	0.01142	0.42495
City 02	850	18	0.37648	0.34329	0.15009	0.00231	0.01141	0.91474
	650		0.16682	0.11762	0.06568	0.00053	0.00987	0.74450
	550		0.13161	0.14171	0.05146	0.00029	0.00491	0.86299
Road 01	850	17	0.41358	0.20619	0.15628	0.00300	0.01439	0.84973
	650		0.19967	0.11483	0.08676	0.00099	0.01052	0.78157
	550		0.14202	0.10522	0.04570	0.00023	0.00486	0.84503
Road 02	850	12	0.27568	0.33470	0.09737	0.00104	0.00583	0.95428
	650		0.15556	0.15142	0.03018	0.00016	0.00386	0.86970
	550		0.19128	−0.01455	−0.00521	0.00021	0.01277	0.01266
Rice Filed 01	850	15	0.53679	0.27827	0.09616	0.00181	0.02338	0.55385
	650		0.11970	0.18270	0.03156	0.00038	0.01003	0.44851
	550		0.10127	0.17415	0.01844	0.00017	0.00499	0.66483
Rice Filed 02	850	17	0.42183	0.97034	0.09536	0.00509	0.01776	0.88423
	650		0.08479	0.19337	0.01879	0.00029	0.00832	0.61665
	550		0.11525	0.20570	0.03976	0.00044	0.00901	0.72705
Rice Filed 03	850	16	0.67447	0.52983	0.18847	0.00579	0.02538	0.79729
	650		0.06865	0.36344	0.03048	0.00165	0.02284	0.55617
	550		0.11149	0.25693	0.06119	0.02578	0.01440	0.71161
Forest 01	850	14	0.39151	0.80804	0.20109	0.00766	0.01748	0.93890
	650		0.05900	0.27816	0.02135	0.00031	0.00532	0.83414
	550		0.09240	0.19465	0.02910	0.00026	0.00251	0.96595
Forest 02	850	19	0.40745	0.30062	0.14674	0.00207	0.00978	0.93156
	650		0.02354	0.14556	0.00650	0.00008	0.00320	0.82623
	550		0.01128	0.22945	0.00787	0.00019	0.00418	0.84484
Forest 03	850	19	0.35001	0.47114	0.19200	0.00654	0.04461	0.63454
	650		0.04038	0.18179	0.02518	0.00026	0.00919	0.56517
	550		0.07844	0.15586	0.02914	0.00026	0.00919	0.60143
Orchard 01	850	17	0.31021	0.81239	0.18977	0.00562	0.03055	0.79459
	650		0.06669	0.08811	0.01563	0.00019	0.00979	0.18653
	550		0.06282	0.18447	0.02003	0.00027	0.01004	0.38580
Orchard 02	850	13	0.36488	0.30892	0.12318	0.00273	0.03051	0.49198
	650		0.13335	0.10234	0.03517	0.00044	0.01400	0.25455
	550		0.09354	0.14928	0.02295	0.00037	0.01290	0.22041
Orchard 03	850	19	0.37672	0.45538	0.18425	0.00470	0.01699	0.90232
	650		0.08293	0.11196	0.02230	0.00014	0.00491	0.75156
	550		0.10429	0.16293	0.03404	0.00028	0.00565	0.81334
Vineyard 01	850	7	0.44287	0.30410	0.13808	0.00075	0.00420	0.90726
	650		0.10222	0.13384	0.03386	0.00011	0.00698	0.38347
	550		0.11916	0.07852	0.02431	0.00003	0.00330	0.56005
Vineyard 02	850	9	0.29525	0.66067	0.21020	0.00322	0.01086	0.94991
	650		0.23529	−0.05420	0.06330	0.00036	0.00638	0.84570
	550		0.09935	0.23661	0.07060	0.00037	0.00425	0.93742
Vineyard 03	850	18	0.52170	0.31249	0.18596	0.00414	0.01692	0.91498
	650		0.13798	0.05623	0.04880	0.00040	0.01116	0.48548
	550		0.13069	0.07639	0.03002	0.00015	0.00595	0.64939

to be continue

Surface	Band[nm]	N_{obs}	K_0	K_1	K_2	σ_{obs}	RMS_{dif}	R^2
Marsh 01	850	18	0.29545	0.21139	0.04664	0.00039	0.00786	0.35603
	650		0.03647	0.16461	0.01434	0.00010	0.00336	0.81186
	550		0.07366	0.17796	0.03467	0.00022	0.00523	0.80990
Marsh 02	850	8	0.08848	0.68227	0.18535	0.00125	0.00656	0.95351
	650		0.05602	0.06820	−0.01677	0.00005	0.00250	0.75084
	550		0.07531	0.13012	0.00269	0.00013	0.00705	0.44235

N_{obs}: Number of available multiangular points, K_0, K_1, K_2, : Fitting parameters,

R^2: Coefficient of determination.

The BRDFs for water surface covers are isotropic with respect to the viewing zenith angle.

We can compute the spectral BRDFs for target surface covers based on the results in Table 1. The spectral BRDFs for two target surface covers are shown in Fig. 1. The shape of BRDFs for River 01 and Forest 01 are 3 dimensionally presented in Fig. 1 (a), and(b), respectively. Fig. 1(a) shows that the spectral BRDFs for River is very flat at all three wavelengths (550nm, 650nm and 850nm) and they obey a Lambert reflection law. We can notice from Fig. 1(b) that the BRDF for Forest is nearly flat against the viewing zenith angle at 550nm and 650nm, with showing a very slight increase in the back scattering direction, whereas it shows clearly a large albedo increase (hot spot) in the back scattering direction at 850nm.

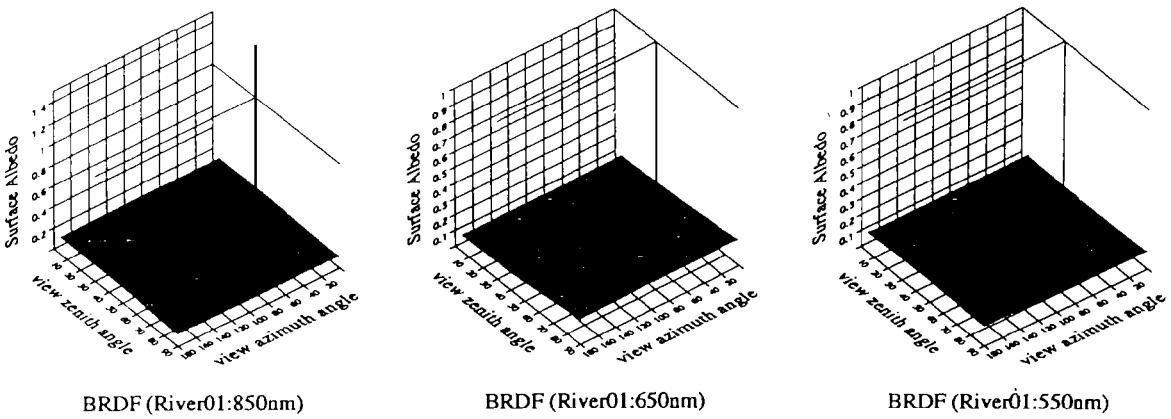

Fig. 1(a) The spectral BRDFs for river 01

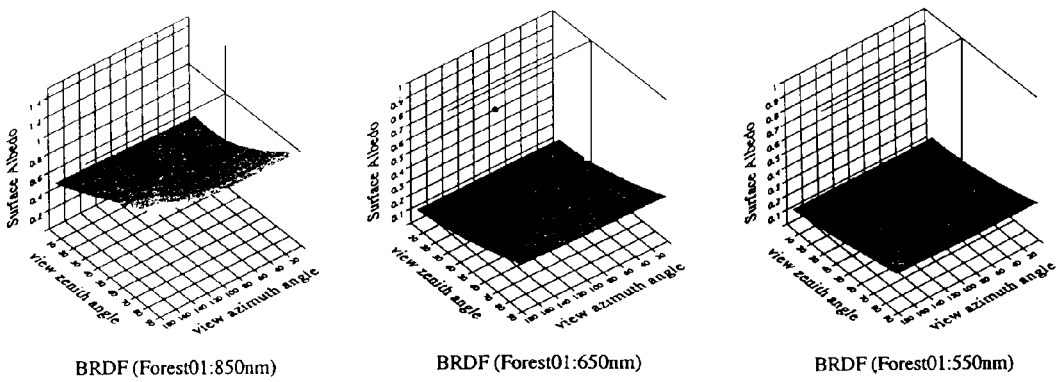

Fig. 1(b) The spectral BRDFs for Forest 01

6 CONCLUSIONS

Previous paper by Deuzé *et al.*[6] derived a simple empirical model for the BRDF and they tabulated three coefficients k_0, k_1 and k_2 for 11 different surface covers. We found that our estimated values of them do not agree well with their values. One major reason for this poor agreement is because of their inaccurate estimation of surface albedos. Since they account only for the first-order Rayleigh scattering, their estimated reflectances for "River Water", "Forest", and "Rice Field" are overestimated by about 4%—9% at 850nm and about 5%—7% at 550nm, when compared with our results in which multiple scatterings by Rayleigh and aerosol particles are taken into account. In this study, the estimation of the spectral BRDFs for selected land covers was made using the airborne POLDER image data. We found that the Lambert reflection law can be a valid BRDF for water surface covers at 550nm, 650nm, and 850nm. However, the Lambert law is not an appropriate BRDF for the vegetated surface covers. Finally, the usefulness of multi-angular reflectance observations should be pointed out, together with the importance of the atmospheric correction.

We would like to express our deep appreciation to Profs. Herman and Deschamps at LOA, Universite des Sciences et Technologies de Lille, France and Dr. Bréon at Laboratoire de Modelisation du Climat et de l'Environment, France for kindly providing the Medimar POLDER data. This study was supported by the Research Contract No. NASDA-PSPC-18282, National Aeronautics and Space Development Agency of Japan.

REFERENCES

[1] Deschamps, P. M., Bréon, F. M., Leroy, M., Podaire, A., Bricaud, A., Buriez, J. C., Sèze, G. The POLDER mission: instrument characteristics and science objectives. *IEEE Trans. Geosci. Remote sensig*, 1994, **32**(3): 598—615.

[2] J. L. Deuze *et al*. Analysis of the POLDER Airborne Instrument Observations over Land Surfaces. *Remote. Sens. Environ.*, 1993, **45**: 137—154.

[3] Bréon, F. M., Deschamps, P. M. Optical and physical parameter retrieval from POLDER measurements over the ocean using an analytical model. *Remote Sens. Environ.*, 1993, **43**: 193—207.

[4] Kawata, Y. *et al*. Atmospheric correction algorithm for remote sensing data with multi-viewing angles, IGARSS' 93, 1993, 1, 113-1, 115.

[5] Takemata, K., Kawata, Y. Estimation of land surface BRDF by using airborne POLDER image data. *IEICE Trans. Commun.*, 1995, **78**(12): 1, 591—1, 597.

[6] Hansen, J. E., Travis, L. D. Light scattering in planetery atmospheres. *Space Sci. Rev.*, 1974, **13**: 527—610.

[7] Kneizys, F. X., Shettle, E. P., Gallery, W. O., Chetwynd, J. H. Jr., Abreu, L. W., Selby, J. E. A., Clough, S. A., Fenn, R. W. Atmospheric Transmittance/Radiance: Computer code Lowtran-6. Air Force Geophys. Laboratory, Hanscom AFB, MA, Rep. AFGL—TR—83—0187, 1983.

AUTHOR

Yoshiyuki Kawata was born on Jan. 7 1946 and received the B.S. and Sc.D. degrees in Astrophysics from Kyoto University in 1968 and 1978 respectively. He also received the M.S. and Ph.D. degrees in Astronomy from University of Massachusetts, Amherst, Mass. in 1970 and 1974, respectively. From 1974 to 1976 he worked at NASA Goddard Institute for Space Studies, New York, N.Y. as a National Academy of Science resident research associate. In 1976 he joined the Information Science Laboratory, Kanazawa Institute of Techology, as an Associate Professor. Currently, he is a Professor of Environmental Systems Engineering and a Director of the Environmental Information Research Laboratory, Kanazawa Institute of Techology. His research interests are in the areas of remote sensing image processing, numerical simulations on environmental problems and applications of radiative transfer theory in the planetary environment. He has more than 150 publications.

通过航空 POLDER 数据估计地表二向性反射分布函数

Y. Kawata
(Environmental Information Research Laboratory Kanazawa Institute of Technology, Ogigaoka 7-1, Nonoichi, Ishikawa 921, Japan)

K. Takemata
(Department of Electrial Engineering Kanazawa Technical College, Hisayasu 2-270, Kanazawa, Ishikawa 921, Japan)

T. Yonekura
(Environmental Information Research Laboratory Kanazawa Institute of Technology, Ogigaoka 7-1, Nonoichi, Ishikawa 921, Japan)

摘 要 研究中，通过选择目标区的 POLDER 图象数据来估计目标的二向性反射分布函数，其主要结果可简述如下：

1) 我们发展了一种大气纠正算法，它适用于源自 POLDER 传感器的图象数据格式。通过这种算法，将连续的不同视角的 POLDER 陆地图象转化为一系列表面反照率图象，该过程考虑了多次散射。

2) 然后，选定 21 个目标区，包括河流、水塘、城市、道路、森林等，其光谱二向性反射分布函数通过连续的反照率图象来估计。研究发现，水表面的二向性反射分布函数 550nm，650nm，850nm 处呈现朗伯体特征，同时发现有植被覆盖地表的二向性反射分布函数在 550nm 和 650nm 处大致为各向同性，而在 850nm 处则表现为各向异性。该文给出了所有靶区按经验二向性反射分布函数的拟合参数值。

关键词 POLDER，二向性反射分布函数 (BRDF)，大气纠正，多次散射